ADVANCES IN ATMOSPHERIC SCIENCES, VOL. 27, NO. 3, 2010, 583–593

A Regional Air–Sea Coupled Model and Its Application over East Asia in the Summer of 2000

FANG Yongjie (房永杰), ZHANG Yaocun* (张耀存),
TANG Jianping (汤剑平), and REN Xuejuan (任雪娟)

School of Atmospheric Sciences, Nanjing University, Nanjing 210093

(Received 15 December 2008; revised 30 June 2009)

ABSTRACT

A regional air–sea coupled model, comprising the Regional Integrated Environment Model System (RIEMS) and the Princeton Ocean Model (POM) was developed to simulate summer climate features over East Asia in 2000. The sensitivity of the model's behavior to the coupling time interval (CTI), the causes of the sea surface temperature (SST) biases, and the role of air–sea interaction in the simulation of precipitation over China are investigated. Results show that the coupled model can basically produce the spatial pattern of SST, precipitation, and surface air temperature (SAT) with five different CTIs respectively. Also, using a CTI of 3, 6 or 12 hours tended to produce more successful simulations than if using 1 and 24 hours. Further analysis indicates that both a higher and lower coupling frequency result in larger model biases in air–sea heat flux exchanges, which might be responsible for the sensitivity of the coupled model's behavior to the CTI.

Sensitivity experiments indicate that SST biases between the coupled and uncoupled POM occurring over the China coastal waters were due to the mismatch of the surface heat fluxes produced by the RIEMS with those required by the POM. In the coupled run, the air–sea feedbacks reduced the biases in surface heat fluxes, compared with the uncoupled RIEMS, consequently resulted in changes in thermal contrast over land and sea and led to a precipitation increase over South China and a decrease over North China. These results agree well observations in the summer of 2000.

Key words: regional, air–sea coupled model, coupling time interval, air–sea interactions, East Asian climate

Citation: Fang, Y. J., Y. C. Zhang, J. P. Tang, and X. J. Ren, 2010: A regional air–sea coupled model and its application over East Asia in the summer of 2000. *Adv. Atmos. Sci.*, **27**(3), 583–593, doi: 10.1007/s00376-009-8203-7.

1. Introduction

Regional Climate Models (RCMs) have experienced a period of rapid development since their appearance in the late 1980s (Dickinson et al., 1989; Giorgi and Bates, 1989; Giorgi et al., 1996; Fu et al., 2000; Pal et al., 2007). Owing to their better description of terrain features and underlying surface conditions, and incorporation of detailed land–surface processes, RCMs can be used to capture regional-scale characteristics of temperature and precipitation, as well as the impact of soil moisture variation on the regional climate (Kim and Hong, 2007). These features and their effects are not well represented in General Circulation Models (GCMs) due partly to the coarse resolution and simplified physical process schemes used in GCMs. Considering the importance of RCMs in regional climate studies, more and more research groups have been involved in the development of RCMs, attempting to make RCMs more suitable for the simulation of the unique climate features over East Asia (Liu et al., 1996; Liu and Ding, 2001; Leung et al., 2004; Ding et al., 2006; Qian and Leung, 2007).

In recent years, the global change System for Analysis, Research and Training Regional Center for Temperate East Asia (START TEA) has carried out a series of studies on the development and application of RCMs (Zhang et al., 2005; Feng and Fu, 2006) and established the Regional Integrated Environment Model System (RIEMS) (Fu et al., 2000; Fu and Su, 2004).

*Corresponding author: ZHANG Yaocun, yczhang@nju.edu.cn

Preliminary validation and application work for the RIEMS has shown that it has a moderate ability in simulating mean climate state, extreme events, and climate changes over East Asia (Xiong et al., 2003; Wu et al., 2004; Xiong, 2004; Xiong et al., 2006). However, there are still several drawbacks and limitations in the RIEMS, such as its overestimation of precipitation over most areas of China, especially North China. Moreover, SSTs in the coastal oceans are specified by the observed SST as the ocean boundary condition in the RIEMS, which is a fixed external forcing condition. Although the atmospheric response to oceanic forcing is included, the model fails to treat air–sea interactions and cannot represent reasonably the strong feedback between ocean and regional climate. Therefore, it is necessary to couple the RIEMS with an oceanic model to improve its simulation ability. This served as the primary motivation for the present study.

As part of the development work of the RIEMS, a regional air–sea coupled model system comprising the RIEMS and the Princeton Ocean Model (POM) (Blumberg and Mellor, 1987) was developed and is reported on in this paper. The coupled model is applied to investigate whether and how the coupling improves the simulation of climate features, especially precipitation over East Asia in the summer of 2000. At that time, a catastrophic drought occurred over North China. It is one of the most famous drought disaster cases in China in the last 40 years due to the very small amount of precipitation, its long-lasting duration, and the resulting large economic losses (Wei et al., 2004).

In the coupled model system, the frequency at which information is exchanged between the atmosphere and ocean components is determined by the coupling time interval (CTI). The CTI in global atmosphere–ocean coupled models (CGCMs) has a distinctive impact on the simulation of intraseasonal variations, such as the Madden-Julian Oscillation, and interannual variability, such as ENSO events (Bernie et al., 2005; Danabasoglu et al., 2006). Previous studies have shown that a CTI of one day is an optimal choice for most CGCMs (Danabasoglu et al., 2006; Randall et al., 2007). However, less attention has been paid to the sensitivity of a model's behavior to the CTI in a regional air–sea coupled system (Ren and Qian, 2005; Seo et al., 2007). In the present study, a group of experiments was carried out to focus on this question.

Another key question addressed in this paper relates to "climate drift" occurring both in the early version of CGCMs (Moore and Gordon, 1994) and in regional air–sea coupled models, especially in terms of SSTs, i.e. SST bias (Ren and Qian, 2005). Many studies have investigated the reasons behind SST drift in CGCMs during the past 20 years. The results have shown that a coarse atmospheric or oceanic model, imprecise physical parameterizations (Moore and Gordon, 1994), or some feedback processes (Cai and Gordon, 1999) might contribute to SST drift. Here, we designed a set of coupled model experiments to explore the causes of SST drifts, i.e. SST bias between the coupled and uncoupled simulations. By doing this, we can provide guidance for the future development and optimization of the coupled model system, as well as the RIEMS.

The remainder of the paper is organized as follows. Section 2 introduces the oceanic and atmospheric models and describes the coupling technique. Section 3 briefly describes the numerical experiment schemes. Section 4 presents experiment results with varied CTIs. Section 5 discusses the differences between coupled and uncoupled simulation results. And finally, section 6 provides discussion and a summary.

2. Regional coupled models and coupling technique

The RIEMS was developed by START TEA (Fu et al., 2000), which is a primitive equation, grid point limited area model with hydrostatic compressible balance written in a terrain-following coordinate system. It is an augmented version of the National Center for Atmospheric Research (NCAR) Penn State Meso-scale Model, MM5. A number of physical parameterizations were coupled into the RIEMS, which include a widely used land surface scheme, namely the Biosphere–Atmosphere Transfer Scheme (BATS) (Dickinson et al., 1986), a Holtslag explicit planetary boundary layer formulation (Holtslag et al., 1990), a Grell cumulus parameterization (Grell, 1993), and a modified radiation package (CCM3).

The POM was developed in the late 1970s by G. Mellor's group at Princeton University. It is a sigma-coordinate, free-surface, primitive equation oceanic model. The version of POM used in this modeling system was improved by Chu and Chang (1997) and Qian et al. (1998). The improved POM has delivered good performance in simulating the intraseasonal, seasonal, and annual variation of SST and circulation in the East Asian coastal regions, and can be used to examine the responses of the regional ocean to the East Asian monsoon (Zhang and Qian, 1999; Ren and Qian, 2000a, b; Qian and Wang, 2000).

To couple the atmospheric model with the oceanic model, a flux–SST coupler was used to bridge the two models, in which the RIEMS provides surface heat and momentum fluxes for the POM, and the POM model feeds back SST to the atmospheric component. The coupling simulation begins with the atmospheric

model running for one CTI with observed SST. Then, surface fluxes of momentum, sensible heat, latent heat and radiation are calculated in the atmospheric model and transferred to the oceanic model. Following that, the oceanic model is also integrated for one CTI, and the generated SST is passed to the atmospheric model, which drives another CTI for the atmospheric model. No flux adjustment is included in the coupled model.

3. Numerical experimental design

The RIEMS and POM share the same model domain, which covers most of the East Asian monsoon region centered at 24°N, 121°E (Fig. 1). The horizontal resolution of both the atmospheric and oceanic models is 60 km, with a 115×98 grid in the east-west and north-south directions. The simulation period for both the atmosphere and ocean component was from 25 April to 1 September 2000. For convenience of analysis, we divided the whole China region into four subregions according to regional climate features: Southeast China, North China, Northeast China, and West China (Fig. 1). Also indicated in Fig. 1 are two subregions used for the analysis of the oceanic elements, which include the South China Sea (SCS) and part of the western Pacific warm pool.

NCEP–NCAR reanalysis data II at 6-hour intervals (Kalnay et al., 1996) were used to provide both the initial and lateral boundary conditions for the atmospheric model. The lateral boundary conditions that forced the oceanic model were derived from the climatological mean temperature and salinity data of Levitus (1982) and the non-gradient extrapolation method was used to give the lateral boundary condition of ocean current. Following Ren and Qian (2000a, b), the spin-up integration of the oceanic model included two steps. First, starting from a static ocean, the oceanic model was integrated from 1 January for one year,

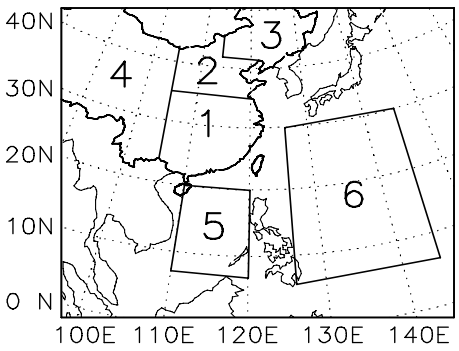

Fig. 1. Model domain and sub-regions. Numbers from 1 to 6 indicate Southeast China, North China, Northeast China, West China, SCS, and part of the western Pacific warm pool, respectively.

forced by NCEP–NCAR reanalyzed monthly wind stress and heat fluxes averaged over the period 1986–2005. Second, the oceanic model was continuously driven to 25 April of the following year, using NCEP–NCAR reanalysis data from 2000. After these two steps, the whole ocean reaches a relatively equilibrium state, and is realistic in terms of its closeness to observed results. Therefore, the outputs of the second step on 25 April 2000 were set as the initial fields of the oceanic model in the coupled system.

Reported in this paper are the results of several simulations performed from 25 April to 1 September 2000. The experiment denoted as CTR_RIEMS was carried out by the RIEMS only, using weekly reanalysis SST as the oceanic boundary forcing, and the experiment denoted as CTR_POM was carried out with the POM only, forced by NCEP–NCAR reanalysis data. In order to examine the responses of the coupled model to the CTI, five experiments of the regional coupled model system with CTIs of 1, 3, 6, 12, and 24 hours were carried out, and denoted as CPL1, CPL3, CPL6, CPL12, and CPL24, respectively. To investigate the causes of SST bias, two other sensitivity experiments were also performed and the related detail will be discussed in section 5.1.

4. Experimental results with varied CTIs

In this section, the analysis focuses on the following two aspects: first, the performance of the coupled model in simulating summer climate features and the oceanic element in 2000; and second, the response of the coupled model to the different CTIs. The simulation results are compared with both reanalysis data and station data. Precipitation and surface air temperature were derived from the World Meteorological Organization surface networks at 160 stations in China. NCEP–NCAR reanalysis data II are used to validate the simulated atmospheric circulation and surface heat fluxes in the interior of the model domain.

4.1 *Simulations of sea surface temperature with varied CTIs*

Figure 2 shows the summer SST distribution for the observation and the coupled simulations with five different CTIs. As demonstrated in Fig. 2f, observed SST is higher than 29°C in waters south of 20°N, except in the middle of the SCS where a cool tongue (<29°C) is located. Overall, the coupled simulations with different CTIs can successfully reproduce high SST regions in the SCS and part of the western Pacific warm pool (Figs. 2a–e). However, the simulated SSTs are cooler than observed in the middle of the Philippine Sea and part of the western Pacific warm

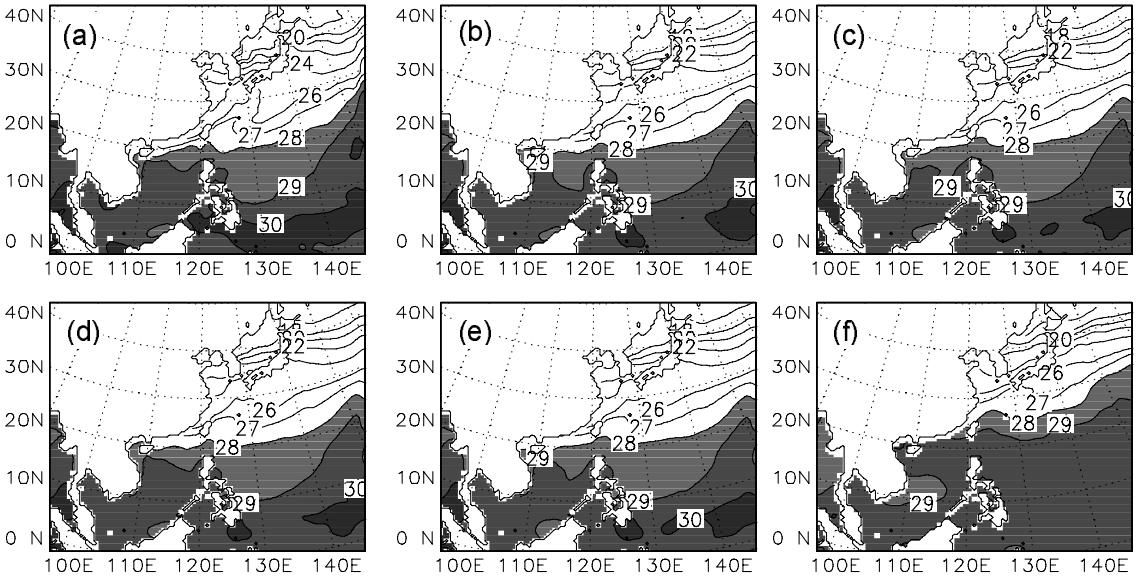

Fig. 2. Distribution of summer SST for: (a) CPL1; (b) CPL3; (c) CPL6; (d) CPL12; (e) CPL24; and (f) observation (units: °C; shading indicates >28°C, 29°C, and 30°C).

pool, and slightly warmer in the east of the SCS and south of the Philippine Sea.

To further examine the sensitivity of SST in the coupled simulations to the CTI, we calculated the root mean square errors (RMSEs) and spatial correlation coefficients (SCCs) of SST in August between the model simulations and observations. These results are summarized in Table 1 and Table 4, respectively. In the whole of China's coastal waters, the RMSEs for CPL6 and CPL12 are 1.09°C and 1.08°C, respectively. These values are slightly smaller than those for CPL1, CPL3, and CPL24, which are 1.26, 1.22, and 1.13°C, respectively (Table 1). The SCCs for CPL3, CPL6, and CPL12 are 0.852, 0.850, and 0.844, respectively. These correlation coefficients are slightly higher than those for CPL1 and CPL24, which are 0.815 and 0.813, respectively (Table 2). The SST RMSE in the other two sub-regions (the SCS and part of the western Pacific warm pool) shows similar characteristics as that in the whole of China's coastal waters. This indicates that the coupled model using a CTI of 3, 6, or 12 hours tends to capture the SST pattern more reasonably than if using 1 or 24 hours.

4.2 *Simulations of precipitation with varied CTIs*

Precipitation is a major criterion when evaluating the performance of global and regional atmospheric models. The simulated and observed summer precipitation in 2000 is presented in Fig. 3. As shown in Fig. 3f for the observed summer precipitation, there are two major rain belts and one rainfall center located in the Huaihe River valley, Southeast China, and Southwest China, respectively. All of the precipitation patterns in the five experiments (Figs. 3a–e) are reasonable when compared with observed results, especially for the two rain belts and one rainfall center. The simulations also capture less precipitation events over North China, compared with the three areas with heavy precipitation mentioned above. However, the simulated precipitation is overestimated across the whole China, and especially in South China. For example, the maximum precipitation rate in all five coupling experiments is around 13 mm d^{-1}, which is about 6 mm higher than observed. Another difference between the simulations and observed results is that the simulated rain belt over the coast of Southeast China is positioned far-

Table 1. The RMSEs between simulated and observed SST in August over the SCS, part of the western Pacific warm pool, and the whole of China's coastal waters (units: °C).

	RMSE				
Region	CPL1	CPL3	CPL6	CPL12	CPL24
China's coastal waters	1.26	1.22	1.09	1.08	1.13
SCS	0.70	0.57	0.51	0.53	0.55
Part of the western Pacific warm pool	0.75	0.65	0.60	0.62	0.67

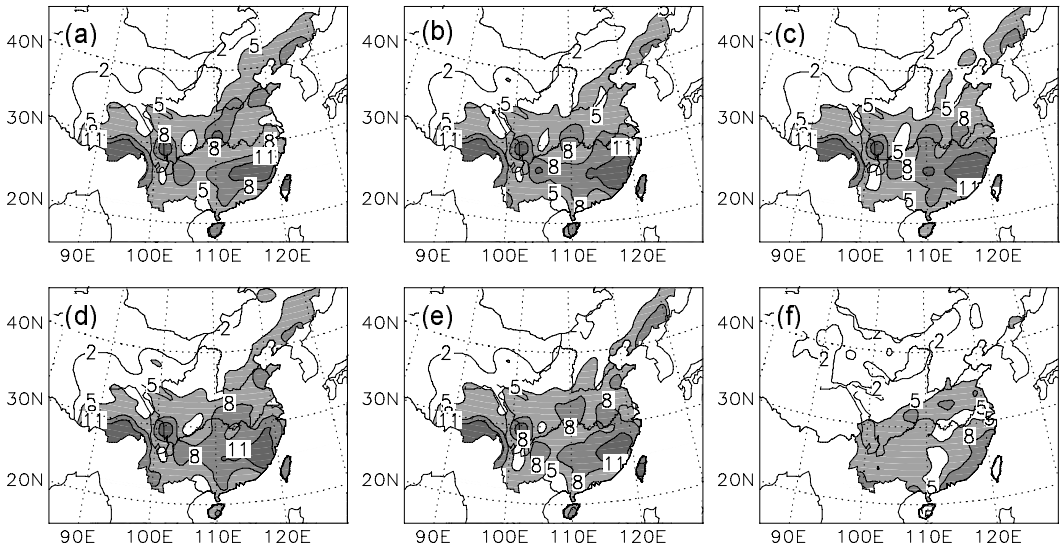

Fig. 3. As in Fig. 2, except for summer precipitation (units: mm d^{-1}; shading indicates > 5, 8, and 11 mm d^{-1}).

ther north than observed. In addition, there are obvious differences among all the five experiments. For example, the northeast-southwest-oriented rain belt over the Huaihe River valley is captured better in CPL3, CPL6, and CPL12 than in CPL1 and CPL24.

Table 2 and Table 3 illustrate the SCCs and RMSEs of precipitation in August between the model simulations and the observation. It is found that, across the whole of China, the SCC in CPL6, with a value of 0.405, is higher than in the other experiments (Table 2), and that the RMSE in CPL3, with a value of 4.66 mm, is smaller than in the other experiments (Table 3). Similar to the analysis on SST in section 4.1, the three simulations of CPL3, CPL6 and CPL12 with CTIs of 3, 6, or 12 hours, present smaller RMSEs than those of CPL1 and CPL24 with CTIs of 1 or 24 hours in most of the sub-regions (Table 3).

4.3 *Simulations of surface air temperature with varied CTIs*

The climatological characteristics of observed summer surface air temperature (SAT) (figure not shown) show a cool center over the Tibet Plateau, a warm tongue over eastern China, and a high temperature belt over the low-latitude ocean region. The five experiments with varied CTIs all capture this distribution pattern, compared with the observation, especially for the warm tongue over eastern China (figure not shown). However, the simulated SAT is overestimated in eastern China and the SCS and underestimated in West China and part of the western Pacific warm pool.

Comparisons of SAT in August between modeled and observed results are given in Tables 4 and 2. It is found that, across the whole of China, the SCCs in the five experiments are mostly the same (Table 2), but the RMSE in CPL6, with a value of 3.21°C is slightly smaller than in CPL1 and CPL24, with values of 3.37°C and 3.34°C, respectively (Table 4). The RMSE of SAT in most of the sub-regions shows similar characteristics to that over the whole of China, although its differences among the experiments with different CTIs are relatively small (Table 4).

4.4 *Simulations of sensible and latent heat fluxes with varied CTIs*

The atmosphere and ocean display a continuum in air–sea interaction. Therefore, the highest possible

Table 2. The SCCs between simulated SST over the whole of China's coastal waters, precipitation, and SAT over the whole of China and the observations in August.

	SCC				
	CPL1	CPL3	CPL6	CPL12	CPL24
SST	0.815	0.852	0.850	0.844	0.833
Precipitation	0.322	0.362	0.405	0.366	0.324
SAT	0.923	0.925	0.923	0.924	0.924

Table 3. The RMSEs between simulated and observed precipitation over sub-regions and the whole of China in August (units: mm d^{-1}).

	RMSE				
Region	CPL1	CPL3	CPL6	CPL12	CPL24
China	4.96	4.66	4.72	4.69	4.98
Northeast China	3.27	3.08	3.09	3.19	3.39
North China	5.00	3.41	3.09	3.68	4.66
Southeast China	3.34	3.61	3.80	4.26	3.90
West China	5.43	5.26	5.46	5.14	5.54

Table 4. The RMSEs between simulated and observed SAT over sub-regions and the whole of China in August (units: °C).

	RMSE				
Region	CPL1	CPL3	CPL6	CPL12	CPL24
China	3.37	3.29	3.21	3.35	3.34
Northeast China	2.11	2.23	2.19	1.86	2.33
North China	2.76	2.61	2.62	2.60	2.65
Southeast China	2.68	2.46	2.38	2.58	2.67
West China	3.91	3.84	3.85	3.91	3.86

coupling frequency in a coupled model will best mimic nature. However, from the above analysis of SST, precipitation and SAT, it is noted that the coupled model using CTIs of 3, 6 or 12 hours tends to make better simulations than when using 1 or 24 hours. To better understand the sensitivity of the coupled model's behavior to the CTI, we calculated the biases of the total oceanic surface heat fluxes, as represented by the sum of the sensible and latent heat fluxes in August, between the model simulations and the observation. As shown in Table 5, the biases of the surface heat fluxes between CPL6 and the observation over the whole of China's coastal waters, the SCS, and part of the western Pacific warm pool, are 15.4, 7.2, and 27.5 W m^{-2}, respectively. These values are detectably smaller, compared to 19.5, 19.4, and 34.8 W m^{-2} for CPL1, and 18.6, 15.3, and 34.5 W m^{-2} for CPL24. This clearly indicates that the relatively high coupling frequency in CPL1, despite its best representation of nature, leads to larger biases in latent and sensible heat fluxes than in CPL6. Meanwhile, the relatively low coupling frequency in CPL24 also results in larger biases in latent and sensible heat fluxes than in CPL6, probably due to its poor representation of the frequency in nature. Further analysis of the bias in net incoming solar radiation and outgoing long-wave radiation (figures not shown) shows similar characteristics to those of surface latent and sensible heat fluxes. This suggests that too high or too low a coupling frequency may cause larger model biases in the air–sea heat flux exchange, which might be responsible for the relatively poor simulation results in CPL1 and CPL24.

5. Comparisons between coupled and uncoupled simulations

In the above sections, we have described a regional air–sea coupled model system and examined its performance by comparison between coupled simulations and observed results. We have addressed especially the sensitivity of the coupled model's behavior to the CTI, and it is encouraging that the coupled model system

Table 5. The biases in surface latent heat plus sensible heat fluxes in August between the model simulations and observations over the SCS, part of the western Pacific warm pool, and the whole of China's coastal waters. (units: W m^{-2}).

	BIAS				
Region	CPL1	CPL3	CPL6	CPL12	CPL24
China's coastal waters	19.5	17.8	15.4	17.1	18.6
SCS	19.4	6.7	7.2	11.4	15.3
Part of the western Pacific warm pool	34.8	33.7	27.5	32.2	34.9

shows good performance in simulating summer climate features and oceanic elements for the year 2000. To explore whether and to what extent the air–sea interactions exert an influence on the performance of the coupled model system, we examine now, in this section, the differences between coupled and uncoupled model simulations. The intercomparison discussed in section 4 revealed that the CTI exerts a robust influence on simulated results, and that the coupled model with CTIs of 3, 6, or 12 hours generates more reasonable results. Therefore, in each experiment discussed below, the CTI was set to 6 hours.

5.1 *Comparisons between CPL6 and CTR_POM*

In this section, we are concerned with the differences between the coupled and uncoupled regional oceanic model simulations. The SST differences between CPL6 and CTR_POM, averaged from June to August, are shown in Fig. 4. Similar to the comparison of SST between the coupled model simulations and the observation (Figs. 2a–f), the significant differences are the cooling bias of up to 0.5°C over part of the western Pacific warm pool and the warming bias of up to 0.5°C over the eastern SCS. Moreover, there are also slight warm biases located in the Bohai and Japan Seas. SST is a key factor in the exchange of heat and momentum fluxes between the ocean and atmosphere, through which the atmosphere and ocean interact with each other. Hence, the SST bias in China's coastal waters may lead to the air–sea interaction biases in the coupled model system, which may contaminate the response of the coupled model system in climate change and climate variability experiments. It is thus important to study the causes of the bias in the coupled model system, with the aim being to eliminate that bias.

In our coupled model, the ocean component is driven by the heat and momentum fluxes transferred

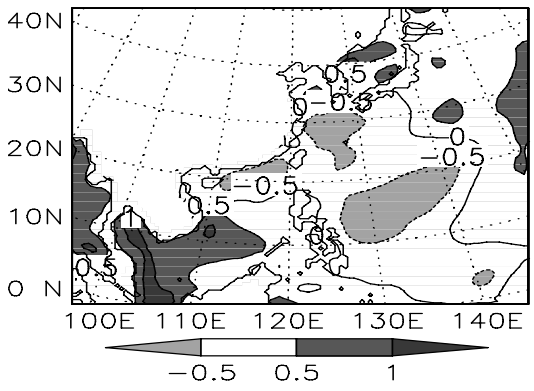

Fig. 4. Summer SST differences between CPL6 and CTR_POM (units: °C).

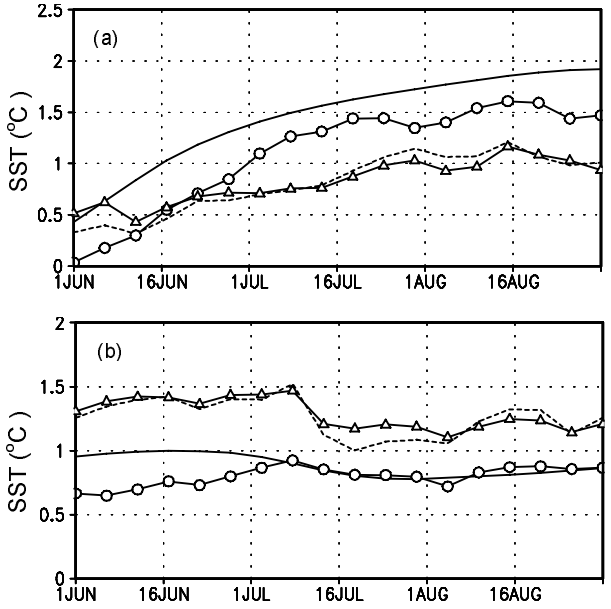

Fig. 5. The time evolution of summer SST in 2000 over (a) part of the western Pacific warm pool and (b) east of the SCS. Solid line, CTR_POM; short dashed line, CPL6; open circles, SENEXP1; open triangle, SENEXP2 (units: +27 °C).

from the atmosphere component. Therefore, the disagreement of these fluxes with those required by the POM might be associated with the simulated SST bias. In order to identify the contribution of the heat and momentum fluxes to the SST bias, two other sensitivity experiments, denoted as SENEXP1 and SENEXP2, were carried out using the coupled system. Both SENEXP1 and SENEXP2 held the same initial and lateral boundary conditions, as well as CTI, as CPL6. However, in SENEXP1 (SENEXP2), the momentum flux (heat flux) forcing the ocean component was taken from the atmospheric component, while the heat flux (momentum flux) was extracted from observations.

Figure 5a shows the time evolution of the simulated SST for CTR_POM, CPL6, SENEXP1, and SENEXP2 from June to August over part of the western Pacific warm pool. It can be seen that the SST differences between CTR_POM and SENEXP1, and between CPL6 and SENEXP2, in which the ocean component is forced by the same heat flux but a different momentum flux, are not robust during the whole simulation period. This indicates that the impact of momentum flux coupling on the cold bias is limited. However, the SST differences between CPL6 and SENEXP1, and between CTR_POM and SENEXP2, in which the ocean component was forced by the same momentum flux but a different heat flux, display a cold tendency during the simulation period. There-

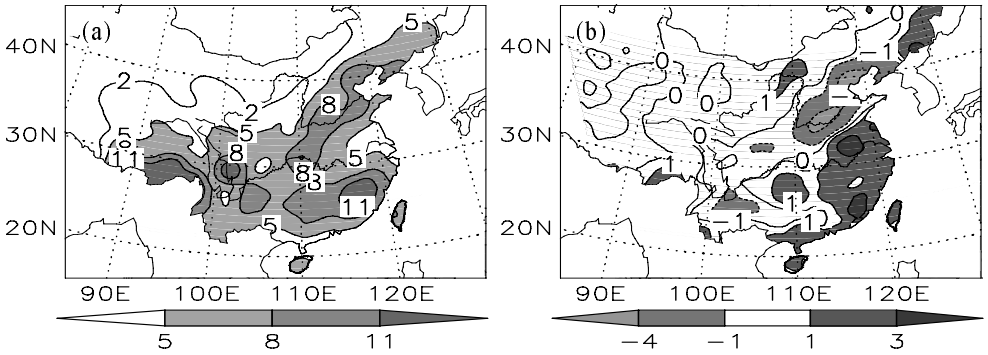

Fig. 6. (a) Distribution of summer precipitation in CTR_RIEMS; (b) differences in summer precipitation between CPL6 and CTR_RIEMS (units: mm d^{-1}).

fore, heat flux coupling plays a much more important role in the cold bias. Similar to Fig. 5a, analysis of Fig. 5b demonstrates the large impact of heat flux coupling on the warm bias over the eastern SCS. The experimental results indicate the necessity to pay more attention to the heat fluxes transferred from the RIEMS, which may not be in agreement with the heat fluxes required by the ocean to maintain the observed climatology.

5.2 *Comparisons between CPL6 and CTR_RIEMS*

Figures 6a and 6b demonstrate the distribution of summer precipitation in CTR_RIEMS and the differences of summer precipitation between CPL6 and CTR_RIEMS. By comparison of the simulated precipitation in the coupled model (see Fig. 3c) and in CTR_RIEMS (see Fig. 6a) with the observation (see Fig. 3f), it is found that both the coupled and uncoupled models systematically overestimate precipitation in North China. When compared with CTR_RIEMS, the coupled model predicts less precipitation, as shown in Fig. 6b, indicating a general improvement in the model performance by coupling with the ocean. In the following analysis, we try to understand how dynamic and thermodynamic coupling in the air–sea interaction system improves precipitation simulation.

The differences of summer surface heat fluxes in 2000 between CPL6 and CTR_RIEMS are shown in Fig. 7a. A noticeable feature is that positive and negative differences of surface fluxes are located to the north and south of 20°N, respectively (see Fig. 7a). The differences of surface heat flux exchanges at the air–sea interface alter the heating rate of the atmosphere (figure not shown), and therefore leads to differences in low-level air temperature (Fig. 7b). As shown in Fig. 7b, an increased temperature belt is elongated from southwest to northeast. Meanwhile, two decreased centers are located in North and Northwest China and the northwestern Pacific, respectively. This pattern indicates changes in thermal contrast over land and sea due to reduced southeast-northwestward temperature gradients over eastern China and opposite changes over the coastal region of eastern China and adjacent open oceans. The differences of low-level atmospheric winds in the summer of 2000 are shown in Fig. 7c. The remarkable differences are a cyclonic and an anticyclonic pattern located over the Sea of Japan and the east of the SCS, respectively, demonstrating that the low-level flow in CPL6 is weaker over most parts of eastern China and stronger over the coastal region of South China. This is consistent with the differences of air temperature gradient at 850 hPa. The northeasterly differential wind dominating mainly over eastern China weakens the transportation of warm and moist air from the south to the north of China, resulting in more precipitation over the Yangtze River valley and Southeast China and less precipitation over North China, as shown in Fig. 6b.

The above analysis shows that the improved simulation of precipitation offered by the coupled modeling approach is largely associated with changes of surface heat fluxes at the air–sea interface over the ocean. Since the changes of surface heat fluxes are extremely sensitive to SST changes, one might wonder whether this improvement comes from the consideration of air–sea interaction or the response of the coupled model to SST biases. As indicated before, the SST biases are attributed to the heat fluxes produced by the RIEMS. Therefore, the discrepancies in the surface heat fluxes between CTR_RIEMS and observations were checked, as shown in Fig. 8. Contrary to the distribution shown in Fig. 7a, CTR_RIEMS exhibits positive biases and negative biases to the south and north of 20°N, respectively, indicating diminished biases of surface heat fluxes in the coupled model. This can be attributed to the new equilibrium state the coupled model reaches after adjusting with the atmospheric model. Upon coupling with the ocean model, the increased surface heat flux cools the local sea surface and weakens the

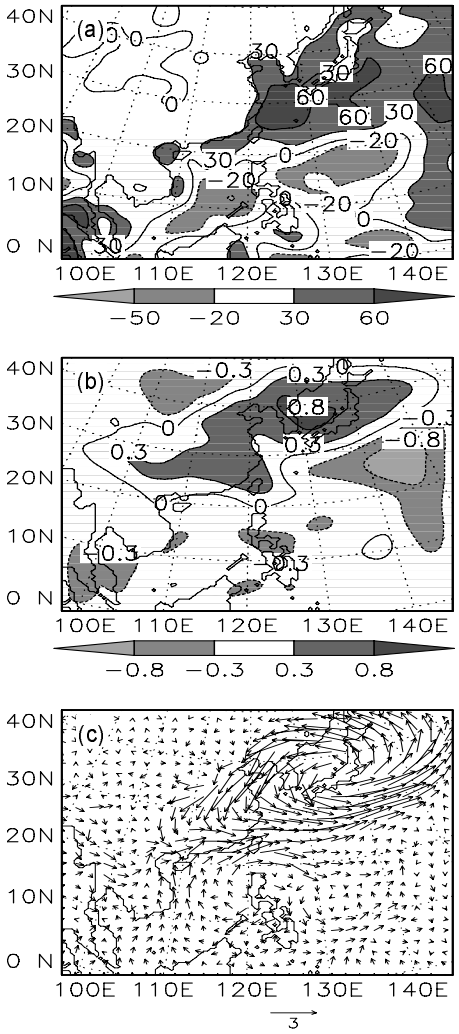

Fig. 7. Differences between CPL6 and CTR_RIEMS in the summer of 2000: (a) surface heat fluxes (units: W m^{-2}, positive means upward); (b) 850 hPa air temperature (units: °C); (c) 850 hPa atmospheric wind (units: m s^{-1}).

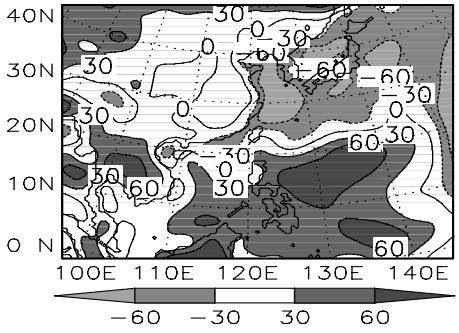

Fig. 8. Discrepancies in surface heat fluxes between CTR_RIEMS and the observation in the summer of 2000 (units: W m^{-2}, positive means upward).

convection activities to the south of 20°N. The lower SST and weaker convection considerably reduce the surface heat fluxes and increase the solar radiation. The case is reversed to the north of 20°N. Therefore, a new equilibrium climate state is established in this air–sea coupled system. The SST is now lower than the observation over part of the western Pacific warm pool, and higher over the Bohai and Japan Seas (see Fig. 4). This indicates that the adjustment of SST to the errors of the atmospheric model leads to improvements in surface heat fluxes, thus resulting in a better simulation of precipitation over China, as illustrated in the analyses above.

6. Discussion and summary

In this study, a regional air–sea coupled model consisting of RIEMS and POM has been constructed. The coupled model has been tested through simulations of climate features in the summer of 2000. Several experiments were carried out, and the behavior of the coupled model examined and compared. The main results are as follows:

(1) Experiments with varied CTIs were performed. It was found that the coupled model, regardless of CTI, can reproduce well the salient features of the East Asian climate in the summer of 2000, including the high SST regions in the SCS and part of the western Pacific warm pool, the rain belts and rain center over the Huaihe River valley, Southeast China, and Southwest China, and a spatial SAT pattern with a cool center, a warm tongue, and a high temperature belt over the Tibet Plateau, eastern China, and low-latitude ocean region, respectively. Comparison studies of SST, precipitation, and SAT in August between the coupled simulations and observed data showed that the coupled model, using a CTI of 3, 6 or 12 hours, tended to produce more successful simulations than if using 1 and 24 hours. Further analysis of surface latent and sensible heat flux biases between coupled simulations and observations showed that both a higher and lower coupling frequency results in larger model biases in air–sea heat flux exchanges over the ocean, which might be responsible for the sensitivity of the coupled model's behavior to the CTI.

(2) Climate drift, especially for SST bias, occurred in the coupled simulation results. Results from sensitivity experiments showed that a possible reason for the cold bias over part of the western Pacific warm pool and warm bias over the eastern SCS is the disagreement in heat fluxes produced by the RIEMS with those required by the POM. Therefore, a more accurate description, revision, and parameterization of the physical process in the RIEMS, especially a good sur-

face heat and momentum flux exchange scheme for the ocean surface, to yield better surface flux estimates, is necessary to remove the SST drift and associated simulation biases.

(3) The coupled model on the regional scale turned out to be a clear improvement compared to the uncoupled run with the atmospheric model, especially for precipitation over North China. This can be attributed to the adjustment of the SST to the errors in the atmospheric model. Upon coupling with the oceanic model, air–sea feedback between the model components reduced biases of surface heat fluxes, compared with the uncoupled RIEMS, consequently resulted in changes in thermal contrast over land and sea and led to a precipitation increase over South China and decrease over North China. These results agree well observations in the summer of 2000.

An important issue that deserves more study is why the coupled model with a higher coupling frequency showed relatively poor performance. Higher coupling frequency might lead to rapid growth of systematic errors in the coupled model, which might therefore be related with the larger model biases in anomalous air–sea heat flux and associated poor simulation results. This needs to be explored further through numerical experiments. In addition, this is a preliminary study emphasizing the importance of regional model air–sea coupling. Long continuous simulations with the coupled model are currently under way to further test the modeling system.

Acknowledgements. This work was supported by the National Basic Research Program under Grand No. 2006CB400506. We are grateful to the anonymous reviewers for their useful suggestions and comments.

REFERENCES

Bernie, D. J., S. J. Woolnough, and J. M. Slingo, 2005: Modeling diurnal and intraseasonal variability of the Ocean Mixed Layer. *J. Climate*, **18**, 1190–1202.

Blumberg, A. F., and G. L. Mellor, 1987: A description of a three-dimensional coastal ocean model. Vol. 4, *Three Dimensional Coastal Ocean Models*, N. S. Heaps, Ed., American Geophysical Union, Washington, D C, 1–16.

Cai, W., and H. B. Gordon, 1999: Southern high-latitude ocean climate drift in a coupled model. *J. Climate*, **12**, 132–146.

Chu, P. C., and C. P. Chang, 1997: South China Sea warm pool in boreal spring. *Adv. Atmos. Sci.*, **14**, 195–206.

Danabasoglu, G., W. G. Large, J. J. Tribbia, P. R. Gent, B. P. Briegleb, and J. C. McWilliams, 2006: Diurnal coupling in the tropical oceans of CCSM3. *J. Climate*, **19**(11), 2347–2365.

Dickinson, R. E., R. M. Errico, F. Giorgi, and G. T. Batest, 1989: A regional climate model for the western United State. *Climate Change*, **15**, 383–422.

Dickinson, R. E., A. Henderson-Sellers, P. J. Kennedy, and M. Wilson, 1986: Biosphere-Atmosphere Transfer Scheme (BATS) for the NCAR community Climate Model. Tech. Note, NCAR/TN-275+STR, National Center for Atmospheric Research, CO, 69pp.

Ding, Y. H., and Coauthors, 2006: Multi-year simulations and experimental seasonal predictions for rainy seasons in China by using a nested regional climate model (RegCM_NCC). Part I: Sensitivity study. *Adv. Atmos. Sci.*, **23**(3), 323–341, doi: 10.1007/s00376-006-0323-8.

Feng, J. M., and C. B. Fu, 2006: Inter-comparison of 10-year precipitation simulated by several RCMs for Asia. *Adv. Atmos. Sci.*, **23**(4), 531–542, doi: 10.1007/s00376-006-0531-2.

Fu, C. B., and B. K. Su, 2004: *The Development and Application of Regional Integrated Enviromental Model System* (*RIEMS*). China Meteorological Press, Beijing, China, 263pp.

Fu, C. B., H. L. Wei, and Y. Qian, 2000: Documentation on Regional Integrated Environmental Model System (RIEMS, Version I). TEACOM Science Report, No. 1, START Regional Committee for Temperate East Asia, Beijing, China, 38pp.

Giorgi, F., G .T. Bates, 1989: The climatological skill of a regional model over complex terrain. *Mon. Wea. Rev.*, **117**, 2325–2347.

Giorgi, F., L. O. Mearns, C. Shields, and L. Mayer, 1996: A regional model study of the importance of local versus remote controls on the 1988 drought and the 1993 flood over the central United States. *J. Climate,* **9,** 1150–1162.

Grell, G. A., 1993: Prognostic evaluation of assumptions used by cumulus parameterization. *Mon. Wea. Rev.*, **121**, 764–787.

Holtslag, A. A. M., E. I. F. de Bruijin, and H. L. Pan, 1990: A high resolution air mass transformation model for short range weather forecasting. *Mon. Wea. Rev.*, **118,** 1561–1575.

Kalnay, E., and Coauthors, 1996: The NCEP/NCAR 40-Year Reanalysis Project. *Bull. Amer. Meteor. Soc.,* **77,** 437–471.

Kim, J. E., and S. Y. Hong, 2007: Impact of soil moisture anomalies on summer rainfall over east Asia: a regional climate model study. *J. Climate*, **20**, 5732–5743.

Leung, L. R., S. Y. Zhong, Y. Qian, and Y. M. Liu, 2004: Evaluation of regional climate simulations of the 1998 and 1999 East Asia summer monsoon using the GAME /HUBEX observational data. *J. Meteor. Soc. Japan,* **82**(6), 1695–1713.

Levitus, S., 1982: *Climatological Atlas of the World Ocean*. NOAA Professional Paper 13, 173pp.

Liu, Y. M., and Y. H. Ding, 2001: Modified mass flux cumulus convective parameterization scheme and its simulation experiment—Part I: Cumulus convection

of the shemes and the sensitivity experiments of MFS. *Acta Meteorologica Sinica*, **59**(2), 129–142. (in Chinese)

Liu, Y. Q., R. Avissar, and F. Giorgi, 1996: Simulation with the regional climate model RegCM2 of extremely anomalous precipitation during the 1991 East Asian flood: An evaluation study. *J. Geophys. Res.,* **101**(21), 26199–26215.

Moore, A. M., and H. B. Gordon, 1994: An investigation of climate drift in a coupled atmosphere–ocean–sea ice model. *Climate Dyn.*, **10**, 81–95.

Pal, J. S., and Coauthors, 2007: The ICTP RegCM3 and RegCNET: Regional climate modeling for the developing world. *Bull. Amer. Meteor. Soc.*, **88**(9), 1395–1409.

Qian, Y., and L. R. Leung, 2007: A long-term regional simulation and observations of the hydroclimate in China. *J. Geophys. Res.*, **112**, D14104, doi: 10.1029/2006JD008134.

Qian, Y. F., B. C. Zhu, and Q. Q. Wang, 1998: Computational scheme of horizontal pressure gradient in ocean models with σ coordinate system. *Journal of Nanjing University*, **34**(6), 691–700. (in Chinese)

Qian, Y. F., and Q. Q. Wang, 2000: Simulate of the annual cycle of the South China Sea temperature by POM. *Chinese J. Atmos. Sci.*, **24,** 373–380. (in Chinese)

Randall, D. A., and Coauthors, 2007: Climate models and their evaluation. *Climate Change 2007: The Physical Science Basis, Contribution of Working Group I to the Fourth Assessment Reoprt of the Intergovernmental Panel on Climate Change.* Cambridge Univesity Press, U.K. and New York, 21pp.

Ren, X. J., and Y. F. Qian, 2000a: Numerical simulations of oceanic elements in the SCS and its neighboring sea regions from January to August in 1998. *Journal of Tropical Meteorology*, **16**, 139–147. (in Chinese)

Ren, X. J., and Y. F. Qian, 2000b: Numerical simulations of seasonal variations of oceanic elements in the SCS and its neighboring sea regions. *Acta Meteorologica Sinica*, **16**, 545–555. (in Chinese)

Ren, X. J., and Y. F. Qian, 2005: A coupled regional air–sea model, its performances and climate drift in simulation of the East Asian summer monsoon in 1998. *International Journal of Climatology,* **25,** 679–692.

Seo, H., A. J. Miller, and J. O. Roads, 2007: The Scripps coupled ocean-atmosphere regional (SCOAR) model, with applications in the eastern Pacific sector. *J. Climate*, **20**, 381–402.

Wei, J., Q. Y. Zhang, and S. Y. Tao, 2004: Physical Causes of the 1999 and 2000 Summer Severe Drought in North China. *Chinese J. Atmos. Sci.*, **28**(1), 125–137. (in Chinese)

Wu, J., W. M. Jiang, C. B. Fu, B. K. Su, H. N. Liu, and J. P. Tang, 2004: Simulation studies of the radiative effect of black carbon aerosol and regional climate responses over China. *Adv. Atmos. Sci.*, **21**(4), 637–649.

Xiong, Z., 2004: The multiyear surface climatology of RIEMS over East Asia. *Climatic and Environmental Research*, **9**(2), 251–260. (in Chinese)

Xiong, Z., C. B. Fu, and Q. Zhang, 2006: On the ability of the regional climate model RIEMS to simulate the present climate over Asia. *Adv. Atmos. Sci.*, **23**(5), 784–791, doi: 10.1007/s00376-006-0784-9.

Xiong, Z., S. Y. Wang, Z. M. Zeng, and C. B. Fu, 2003: Analysis of simulated heavy rain over the Yangtze River Valley during 11–30 June 1998 using RIEMS. *Adv. Atmos. Sci.*, **20**(5), 815–824.

Zhang, Y. C., and Y. F. Qian, 1999: Numerical simulation of the regional ocean circulation in the Coastal Areas of China. *Adv. Atmos. Sci.*, **16**(3), 443–450.

Zhang, Y. J., H. W. Gao, and L. Gerhrd, 2005: Simulation of monsoon seasonal variation of Regional Climate Model REMO in East Asia. *Climatic and Environmental Research*, **10**(1), 41–55. (in Chinese)